

PAPER • OPEN ACCESS

Statistical against dynamical PLF fission as seen by the IMF-IMF correlation functions and comparisons with CoMD model

To cite this article: E.V. Pagano *et al* 2018 *J. Phys.: Conf. Ser.* **1014** 012011

View the [article online](#) for updates and enhancements.

Related content

- [The Manhattan Project: The background](#)
B C Reed
- [Nuclear Materials Science: Nuclear fuel, part 1: fuel and cladding](#)
K Whittle
- [Nuclear Materials Science: Radiation damage](#)
K Whittle



IOP | ebooks™

Bringing together innovative digital publishing with leading authors from the global scientific community.

Start exploring the collection—download the first chapter of every title for free.

Statistical against dynamical PLF fission as seen by the IMF-IMF correlation functions and comparisons with CoMD model

E.V. Pagano¹, L. Acosta^{2,3}, L. Auditore^{2,4}, T. Cap⁵, G. Cardella², M. Colonna¹, E. De Filippo², E. Geraci^{2,6}, B. Gnonno^{2,6}, G. Lanzalone^{1,7}, C. Maiolino¹, N. Martorana^{1,6}, A. Pagano², M. Papa², E. Piasecki^{5,8}, S. Pirrone², G. Politi^{2,6}, F. Porto^{1,6}, L. Quattrocchi^{2,6}, F. Rizzo^{1,6}, P. Russotto¹, A. Trifiro^{2,4}, M. Trimarchi^{2,4} and K. Siwek-Wilczynska⁹

¹INFN Laboratori Nazionali del Sud, Catania, Italy

²INFN Sezione di Catania, Catania, Italy

³Instituto de Fisica, Universidad Nacional Autonoma de Mexico, Mexico

⁴Dipartimento di Scienze MIFT, Universita' Messina, Italy

⁵National Centre for Nuclear Research, Otwock-Swierk, Poland

⁶Dipartimento di Fisica e Astronomia, Universita' di Catania, Italy

⁷Universita' Kore, Enna, Italy

⁸Heavy Ion Laboratory, University of Warsaw, Poland

⁹Faculty of Physics, University of Warsaw, Poland

E-mail: epagano@lns.infn.it

Abstract. In nuclear reactions at Fermi energies two and multi particles intensity interferometry correlation methods are powerful tools in order to pin down the characteristic time scale of the emission processes. In this paper we summarize an improved application of the fragment- fragment correlation function in the specific physics case of heavy projectile-like (PLF) binary massive splitting in two fragments of intermediate mass(IMF). Results are shown for the reverse kinematics reaction $^{124}\text{Sn} + ^{64}\text{Ni}$ at 35 AMeV that has been investigated by using the forward part of CHIMERA multi-detector. The analysis was performed as a function of the charge asymmetry of the observed couples of IMF. We show a coexistence of dynamical and statistical components as a function of the charge asymmetry. Transport CoMD simulations are compared with the data in order to pin down the timescale of the fragments production and the relevant ingredients of the in medium effective interaction used in the transport calculations.

1. Introduction

Two and multi particles intensity interferometry correlation methods are used to extract space-time information about the emission process [1]. Space-time characteristics of light particles (like protons) emission sources are commonly understood in the frame of the Koonin-Pratt equation [2, 3]. For Intermediate Mass Fragments (IMF) relative momentum correlations, large relative momenta are expected due to the strong influence of the long range Coulomb repulsion in the final decay channel. However, also for IMF's correlation functions, information about the reaction mechanism and time scale could be extracted [4, 5, 6, 7, 8, 9, 10]. The coexistence of dynamical and statistical mechanism in the reaction is an important aspect of the Fermi energy



domain where competition between mean field and nucleon-nucleon have to be taken into account in the simulations. First studies using the correlation method were done in the past for central and ternary neck-emissions events with CHIMERA data [11, 12]. In this paper the IMF-IMF correlation function is applied to the physics case as studied by the CHIMERA collaboration, that is the dynamical fission of the projectile-like-fragment (PLF) in $^{124}\text{Sn}+^{64}\text{Ni}$ system at 35 A MeV reverse reaction [13, 14]. The basic idea is to provide a time-scale calibration of the IMF-IMF correlation function in that specific case and to study its shape evolution as a function of the mass asymmetry. Notice that in our physics case the detected pairs of particles (IMFs from PLF fission) are associated with large relative momenta as the ones given by the Coulomb repulsions. As a consequence, our data are compared with simulations including Coulomb trajectories calculations. In this work we present comparisons with the CoMD transport model with different parametrizations of the equation of state of nuclear matter (EOS) [15, 16].

2. Experimental analysis

To select projectile-like fragments of fission-like decay, we restrict our analysis to events with IMFs multiplicity equal to two, having both atomic number Z between 3 and 4. Furthermore, we constrained the IMFs parallel velocity to values greater than 5 cm/ns with respect to the beam axis was. Notice that in the studied system the velocity of the center of mass in the laboratory frame is ≈ 5.2 cm/ns and the projectile velocity is ≈ 8 cm/ns. Complete events were characterized by a total detected parallel momentum greater than 60% of the projectile one and the total collected atomic number Z_{tot} is greater than 40. The charge asymmetry ratio $Z_{Asy} = Z_H / Z_L$ of the emitted pairs of IMFs is in the range: $25 \leq Z_H + Z_L \leq 50$, where Z_H and Z_L are the atomic numbers of the heavy and the light IMF of the pair, respectively. The charge asymmetry is adopted in this paper to classify and characterize the exit channel decay properties. So, in summary the selected set of IMFs was decomposed in three partitions: $1 \leq$

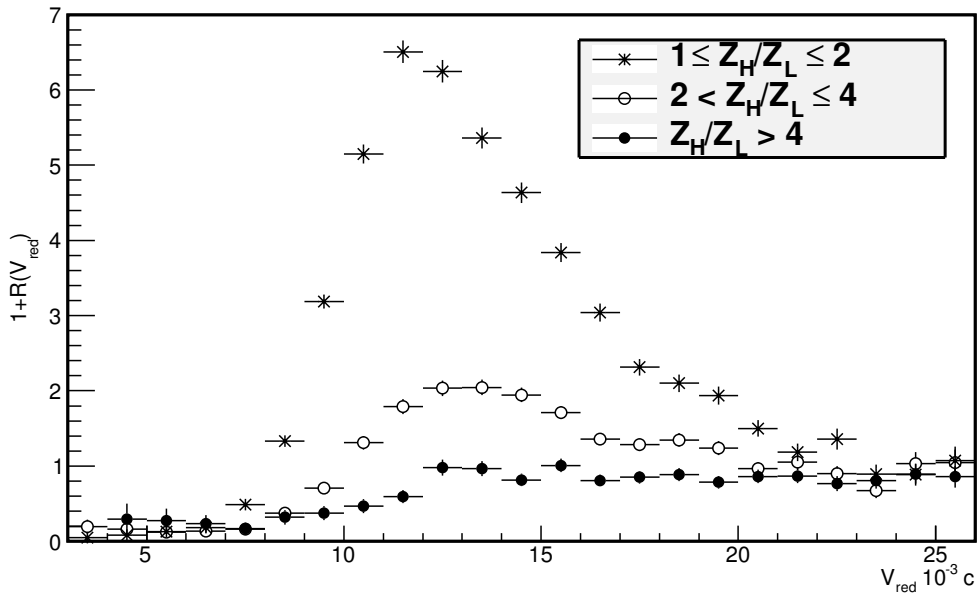


Figure 1. IMF-IMF correlation functions for $25 \leq Z_H + Z_L \leq 50$ gated by different Z_{Asy} condition (see text) [4].

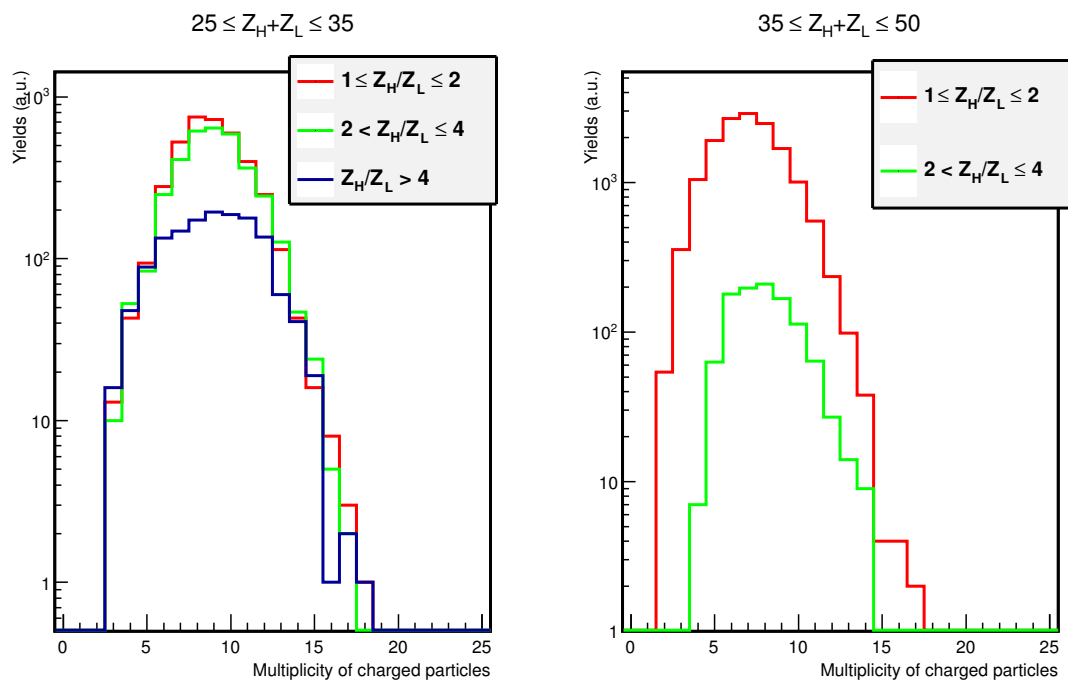


Figure 2. Total charged particles multiplicity as a function of Z_{Asy} , for the two bins of $25 \leq Z_H + Z_L \leq 35$ (left panel) and $35 \leq Z_H + Z_L \leq 50$ (right panel) [4].

$Z_{Asy} \leq 2$, $2 < Z_{Asy} \leq 4$ and $Z_{Asy} > 4$. As it is common, the experimental correlation function

$$1 + R(|\mathbf{V}_{red}|) = C_{12} \frac{Y_{Coinc}(|\mathbf{V}_{red}|)}{Y_{Uncor}(|\mathbf{V}_{red}|)} \quad (1)$$

was evaluated by the ratio between coincident collected pairs of IMFs (in the same event) and uncorrelated ones. The denominator $Y_{Uncor}(|\mathbf{V}_{red}|)$ was computed with the event mixing technique according to Ref. [17]. In our study event mixing computations have been carefully compared with different techniques such as, pseudo singles computations and Montecarlo pseudo-random so mapping the available phase space configuration. However, our analysis is not based on femtoscopy equations like in Refs [2, 18, 19], but was performed by comparisons with transport simulations and the simulated events have been constrained by the same procedures applied to the experimental data. The three IMF-IMF correlation functions, as a function of the three ranges of the Z_{Asy} , are shown in Fig.1 and they have been evaluated as a function of the reduced velocity defined as it follows [6]:

$$\mathbf{V}_{red} = \frac{\mathbf{V}_H - \mathbf{V}_L}{\sqrt{Z_H + Z_L}} = \frac{\mathbf{V}_{rel}}{\sqrt{Z_H + Z_L}} \quad (2)$$

This quantity allows to add together pairs of particles having different atomic numbers [6] in order to increase the statistics that plays a crucial role in such studies. The IMF-IMF correlation functions, for the three ranges of charge asymmetry show very different shapes. Notice that the well-defined bump observed for $1 \leq Z_{Asy} \leq 2$ is centered at a value of the reduced relative velocity that is in agreement with a binary sequential PLF splitting, as it is deduced by the Coulomb repulsion in agreement with the Viola systematics [20]. The energy dissipation has been analysed by inspecting the charged particle multiplicity in the three ranges

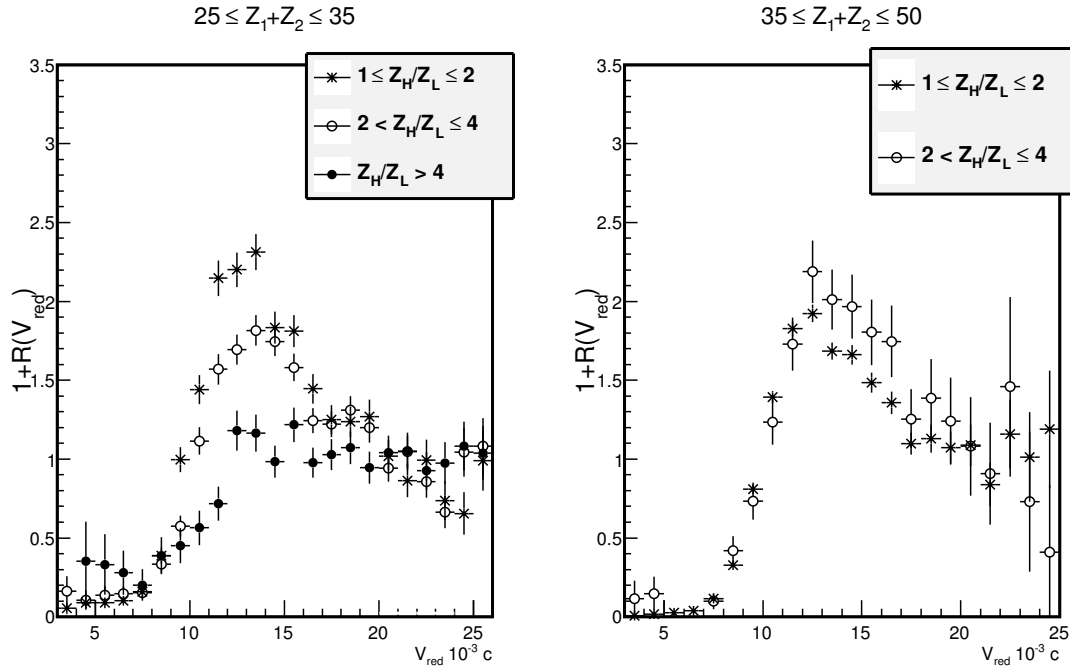


Figure 3. IMF-IMF correlation function for different Z_{Asy} : $25 \leq Z_H + Z_L \leq 35$ (left panel) and $35 \leq Z_H + Z_L \leq 50$ (right panel) [4].

of charge asymmetry and the corresponding sum $Z_H + Z_L$. We evidenced the tendency of the dissipation to grow up with the increase of the asymmetry from a most probable value around 7 charged particles, for the most symmetric gate, up to about 10 charged particles for the most asymmetric one.

In order to achieve a more careful understanding of the different observed shapes (and assuming that the sum $Z_H + Z_L$ is a measure of the size of the emitting source) we improve the class of the selected events with respect to the size of the emitting system and (consequently) the range of the energy dissipation. We have considered two complementary narrower bins of the sum of the atomic number of the two pairs , i.e., one bin defined in the range, $25 \leq Z_H + Z_L \leq 35$ (left panel of Fig.2) and the other one in the range, $35 \leq Z_H + Z_L \leq 50$ (rightpanel of Fig.2).

In Fig.3 the new results for the IMF-IMF correlation functions are shown: in the left panel for the most dissipative range: $25 \leq Z_H + Z_L \leq 35$ and in the right panel for the less dissipative one: $35 \leq Z_H + Z_L \leq 50$. In the first case (larger dissipation) hierarchies in both intensity and shape as a function of the Z_{Asy} are preserved; in contrast, in the second case (lower dissipation) the correlation functions show no significant differences as a function of the Z_{Asy} , (the value of the asymmetry $Z_{Asy} > 4$ is not shown because the statistics was not significant). The natural interpretation is that in the most dissipative range the changing shape of the correlation function is a clear indication of the evolutionary time scale character of the nuclear mechanism leading to the production of the IMFs. Instead, for the most gentle collisions associated with sizes in the range $35 \leq Z_H + Z_L \leq 50$ the space-time configuration is only poorly affected by the asymmetry parameter (practically, both shape and intensity of the correlation functions are unchanged). Once the size of the emitting source was fixed by the value of $25 \leq Z_H + Z_L \leq 35$, the evolution of the intensity and shape of the correlation function vs. the charge asymmetry could be linked to the time scale of the decay process from the prompt dynamical decay (fast process) up to

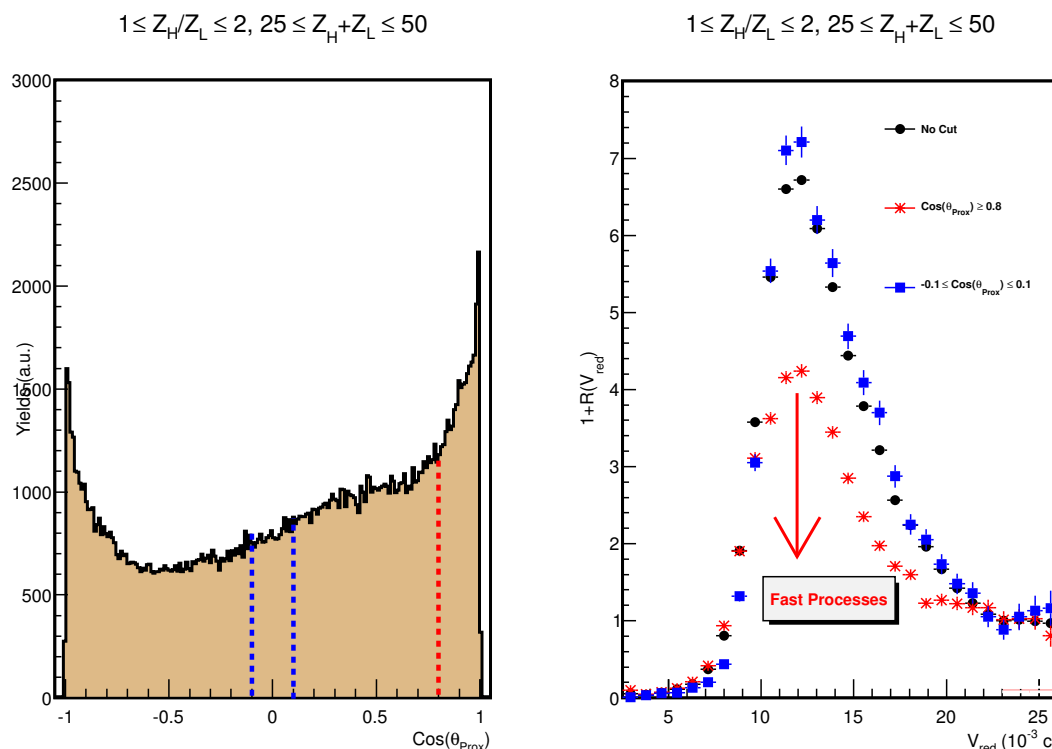


Figure 4. (left panel) distribution of the cosines of θ_{prox} for $25 \leq Z_H + Z_L \leq 50$ and $1 \leq Z_{Asy} \leq 2$. (Right panel) IMF correlation functions with and without constrains in $\cos(\theta_{prox})$.

the equilibrated fission decay (sequential process). The correlation functions were also studied as a function of the theta proximity angle θ_{prox} , which is an independent indicator of both equilibrium emission and dynamical processes [21].

In brief, the theta proximity represents the angular distribution of a selected light IMF of the pair with respect to the reconstructed center of mass vector velocity of the emitting primary PLF source. In the left panel of the Fig.4 the distribution of the $\cos(\theta_{prox})$ for the full range $25 \leq Z_H + Z_L \leq 50$ and for the most symmetric gate of charge asymmetry is shown. In a pure sequential fission decay such a distribution should be forward-backward symmetric with respect to the value of $\cos(\theta_{prox})=0$. So, in agreement with the analysis of refs. [13, 14] the distribution of Fig.4 (left panel) is dominated by equilibrated sequential PLF fission decay and only a small but sizeable contribution ($\approx 10\%$) of it is associated with a prompt dynamical process evidenced by a forward angular asymmetry for the events with a $\cos(\theta_{prox})$ close to 1.

It is very interesting to test the sensitivity the correlation function to the $\cos(\theta_{prox})$ asymmetry. In the right panel of Fig.4 three correlation functions have been evaluated with and without constraints in $\cos(\theta_{prox})$ distribution. All the three correlations are peaked at nearly the same value of the reduced relative velocity (see Fig.1 and text). The correlation function with the largest correlated intensity (blue-full square) corresponds to the one obtained constraining the $\cos(\theta_{prox})$ (bin of 0.2 width) in the range of values $-0.1 \leq \cos(\theta_{prox}) \leq 0.1$ where a pure statistical fission-like sequential decay was evidenced [13, 14] and it is identical (within the accuracy) to the one (black-full dots) corresponding to the total $\cos(\theta_{prox})$ distribution. The third correlation function (red-stars) is calculated constraining the total $\cos(\theta_{prox})$ distribution for values (bin of 0.2 in width as in the black full dots one) $\cos(\theta_{prox}) \geq 0.8$, in the region where the strong

forward-backward asymmetry shows the largest contribution of a dynamical-out of equilibrium fission-like process. It is clearly noticed that the intensity of this latter correlation function is strongly decreased and its shape is broadened; this is a further strong and complementary indication of the high sensitivity of the correlation function to the prompt/dynamical processes.

3. Transport simulations and comparisons

To complete our analysis, we made comparisons between the experimental data and the CoMD model calculations [15, 16]. In Fig.5, e.g., for charge asymmetry in the range, $1 \leq Z_{Asy} \leq 2$, detailed comparisons between the experimental and simulated events of the main experimental observables (a): $Z_H + Z_L$; b): Z_{Asy} and c): $\cos(\theta_{prox})$ distributions) used in this analysis are shown for different parametrization of EOS.

Notice that in CoMDII [15], as already used in the preliminary analysis of refs [4, 5], the sequential decays of the primary fragments have been also included. In CoMDIII [16] simulations and comparisons with experimental data shown in Fig.5 (a), b) and c)) the sequential decay is not included in the simulations. The simulated events have been constrained as the experimental data and, remarkably, the range of the resulting simulated impact parameters, i.e., about $2 \leq b \leq 8$ fm, was found to be consistent with the evaluated experimental one, as deduced by using the Cavata method [22].

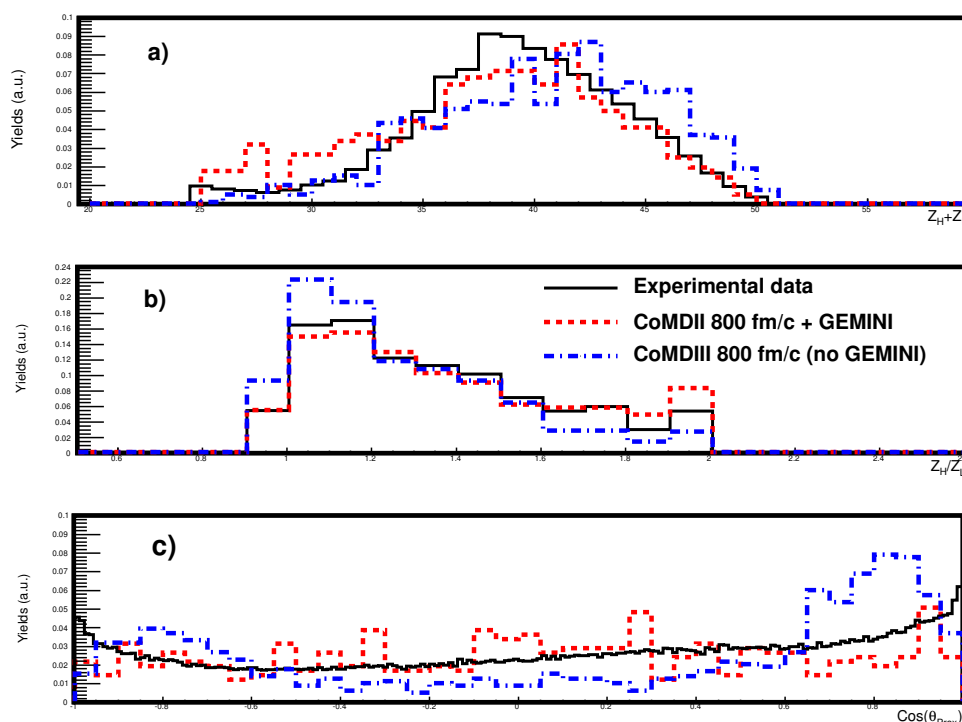


Figure 5. Comparisons between simulated and experimental observables (see text).

In Fig.6 the comparison between the IMF-IMF experimental correlation functions (in the figure the three ranges of Z_{Asy} , like in Fig.1, are reported for simplicity) and the simulated ones for the largest range of the charge sum, $25 \leq Z_H + Z_L \leq 50$ is shown. Full squares (in red) represents a time computation of 800 fm/c in CoMDIII simulations and the full dots (in green) time computation of 650 fm/c. A good agreement between data and simulations is observed for the intermediate and largest asymmetries, indicating that, the case of dynamical breakup/fission

occurring within 800 fm/c is dominated by an asymmetric splitting of intermediate or large charge asymmetries. It is also envisaged to continue the comparison using the CoMD and also with other transport models in order to obtain information on the reaction mechanism and in medium effective interaction that are as much as possible model independent. For instance, a good candidate to simulate dynamical fission processes is the stochastic mean field models, such as SMF and BLOB [23, 24].

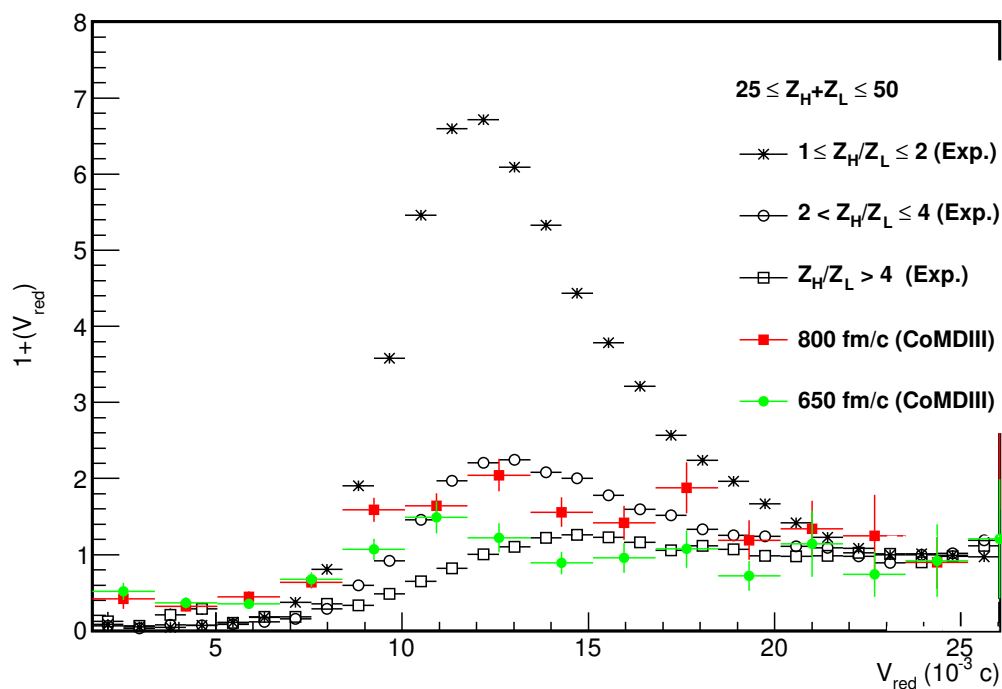


Figure 6. Comparisons between theoretical and experimental correlation functions.

4. Conclusions and future perspectives

In this work a first detailed study of the IMF-IMF correlation functions of particle pairs of both high relative momenta and charges, in the specific case of dynamical PLF fission in the collision $^{124}\text{Sn} + ^{64}\text{Ni}$ at 35 AMeV [14] [13] has been presented. We have shown that the correlation function for massive fragments is a powerful and complementary experimental method in order to pin down on the time scale, size and dissipative mechanism of multiple massive IMF emission in nuclear reactions at Fermi energies. Important sources of information are expected to be available by careful comparisons of experimental data with advanced nuclear dynamics simulations. The results discussed in this paper strongly encourage for further detailed investigations with new exclusive experiments in this field [25].

- [1] Henzl V *et al.* 2012 *Phys. Rev. C* **85** 014606
- [2] Koonin S E 1977 *Phys. Lett. B* **70** 4
- [3] Pagano E V 2013 *Nuovo Cimento C* **36** (issue 4) 9
- [4] Pagano E V *et al.* 2016 *Il Nuovo Cimento C* **39** 404
- [5] Pagano E V A.A. 2016/2017 *Phd Thesis University of Catania*

- [6] Kim Y D *et al.* 1992 *Phys. Rev. C* **45** 338
- [7] Schapiro O, DeAngelis A R and Gross D H E 1994 *Nucl. Phys. A* **568** 333
- [8] Pal S 1995 *Nucl. Phys. A* **594** 156
- [9] Xiao Z G *et al.* 2006 *Phys. Lett. B* **639** 436-440
- [10] Pagano E V *et al.* 2017 *PoS(BORMIO)* 022
- [11] Geraci E *et al.* 2004 *Nucl. Phys. A* **732** 173
- [12] Maiolino C *et al.* 2005 *Proceedings of the XLIII International Winter Meeting on Nuclear Physics, Bormio, edited by Iori I and Bortolotti A* **124** 194
- [13] De Filippo E *et al.* 2005 *Phys. Rev. C* **71** 064604
- [14] Russotto P *et al.* 2010 *Phys. Rev. C* **81** 064605
- [15] Papa M, Maruyama T and Bonasera A 2001 *Phys. Rev. C* **64** 024612
- [16] Papa M 2013 *Phys. Rev. C* **87** 014001
- [17] Lisa M A, Gong W G, Gelbke C K and Lynch W G 1991 *Phys. Rev. C* **44** 2865
- [18] Lednický R and Lyuboshitz V L 1982 *Sov. J. Nucl. Phys.* **35** 770
- [19] Pratt S and Ztang B 1987 *Phys. Rev. C* **6**
- [20] Viola V E, Kwiatkowski K and Walker M 1985 *Phys. Rev. C* **31** 1550
- [21] De Filippo E *et al.* 2012 *Phys. Rev. C* **86** 014610 and references therein.
- [22] De Filippo E and Pagano A 2014 *Eur. Phys. J. A* **50** 32
- [23] Rizzo C *et al.* 2014 *Phys. Rev. C* **90** 054618
- [24] Napolitani P, Colonna M 2016 *EPJ Web of Conferences* **117** 07008
- [25] Defilippo E, Pagano E V, Russotto P *et al.* CHIFAR @LNS, approved proposal.